



Munich Personal RePEc Archive

## **A direct-based method for real-time transient stability assessment of power systems**

Khazaei, Saeed and Hayerikhiyavi, Mohammadali and Montaser Kouhsari, Shahram

Amirkabir University of Technology, Department of Electrical Engineering. Theran, Iran., University of Central Florida, Department of Electrical Engineering. Orlando, USA., Amirkabir University of Technology, Department of Electrical Engineering. Theran, Iran.

28 February 2020

Online at <https://mpra.ub.uni-muenchen.de/101705/>  
MPRA Paper No. 101705, posted 13 Jul 2020 05:47 UTC

# A Direct-Based Method for Real-Time Transient Stability Assessment of Power Systems

Saeed Khazaei<sup>a</sup>, Mohammadali Hayerikhiyavi<sup>b\*</sup>, Shahram Montaser Kouhsari<sup>a</sup>

<sup>a</sup> Amirkabir University of Technology, Department of Electrical Engineering, Tehran, Iran.

<sup>b</sup> University of Central Florida, Department of Electrical Engineering, Orlando, USA.

Keywords	Abstract
Transient stability; direct methods; energy function; critical machines.	Power system stability is a problem that has challenged power system engineers for many years. This paper studies transient stability assessment using direct methods by Equal Area Criterion (EAC) and Transient Energy Function (TEF). It introduces a Stability Margin Index (SMI) for the power systems based on kinetic energy. Firstly, the proposed method calculates the critical angles and the critical kinetic energies for all machines in a power system using EAC method. Next, when a fault occurs, by using TEF and the kinetic energy, the system is divided into two bunches: the Critical Machine Group (CMG), and Non-Critical Machine Group (NCMG). Then, the stability margin of the system is rapidly judged by using the proposed SMI. By this method, the stability of the system in real-time and at any moment is calculated. Due to the simple calculations, low requirement of data and, non-requirement post-fault data, the calculation time in comparison to the other ways in which directly potential energy obtained, is much less and appropriate for real-time applications. The proposed method has been applied to IEEE 9 bus test systems and the results show the usefulness and effectiveness of this method.

## 1. Introduction

Traditionally, off-line dynamic simulations are considered for transient stability assessment. By contrast, the real-time transient stability assessment is using in monitoring the system transients [1]. The first tests of practical power system stability were done in 1925[2, 3]. The stability problems were associated with remote power plants, feeding load centers over long transmission lines[4]. Transient stability methods are further classified into two major categories: direct methods [2-7], numerical methods based on numerical integration [8-10]. Nonlinearities play an overcoming role in large disturbances that take place in a system. To determine transient stability or instability under a large disturbance or cascade disturbances, Time-Domain (TD) method is usually used to solve the set of nonlinear equations describing the system dynamic. The Transient Energy Function (TEF) method [5, 6], and Equal Area Criterion (EAC) [6, 11] have also been used for power system transient stability assessment. These methods were successfully applied to two-machine systems. However, for transient stability assessment, these methods have some modeling restrictions and they need the high value of computations [12]. In his paper rotor angle stability is studied. There is another category of stability which is called voltage stability, which tries to control the voltages at all busbars in the acceptable range [13-16] after disturbance some action does prevent from system's blackout [17]. One of the ways for preventing blackouts and increasing the reliability of the system is system re-configuration by opening breakers [18]. In this paper the proposed method, at first calculates the critical kinetic energy ( $K_{crit}$ ) of each

machine in the power system, using EAC, which is equal to the potential energy of each machine. When the kinetic energy of each machine is found, the system is divided into two groups: the Critical Machine Group (CMG), and the Non-Critical Machine Group (NCMG) and by providing SMI, transient stability of the power system is calculated in real-time until the fault is clear and the stability margin can be determined.

## 2. Model of system

Before developing direct methods, it is essential to introduce the swing equation and model of the system to represent the dynamics of a power system. Mathematically, for each synchronous machine in the power system, the rotor angle  $\delta_i$  ( $i=1,2,\dots,n$ ) in the synchronous reference frame is defined by the swing Eq. (1) and (2) [19]:

$$\frac{d\delta_i}{dt} = \omega_i - \omega_0 \quad (1)$$

$$\frac{d\omega_i}{dt} = \frac{1}{M} [P_{m_i}(t) - P_{e_i}(t)] \quad (2)$$

where,  $M$  is the moment of inertia,  $P_m$  is the mechanical power,  $P_e$  is the electrical power,  $\omega_i$  is the speed of the generator's rotor, and  $\omega_0$  is the speed of the reference generator. The single-machine infinite-bus (SMIB) system shown in Figure 1. The generator is represented by the classical model, which ignores the saliency of the round rotor, for the aim of transient stability. This model only takes into account the transient reactance  $X_d$  in which the direct and quadrature components are equal.

\* Corresponding Author:

E-mail address: mohammad.ali.hayeri@knights.ucf.edu – Tel, (+1) 4076806778

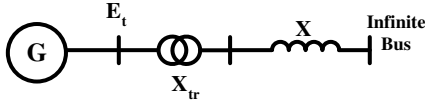


Figure 1. Single-machine infinite-bus system [4].

### 3. Equal-area Criterion

In transient stability, the critical clearing time is important for circuit breakers when the large disturbance occurs in the system [20, 21]. Take into account a single-machine infinite-bus (SMIB) system of Figure 1, it is not necessary to solve the swing equation to determine whether the rotor angle increases indefinitely or oscillates about an equilibrium point [22]. Assume that the system is a purely inductive, a constant  $P_m$ , and constant voltage behind transient reactance for the system in Figure 1. When a 3-phase fault occurs at  $t=0$  and is cleared. The power angle characteristic of the system is shown in Figure 2.

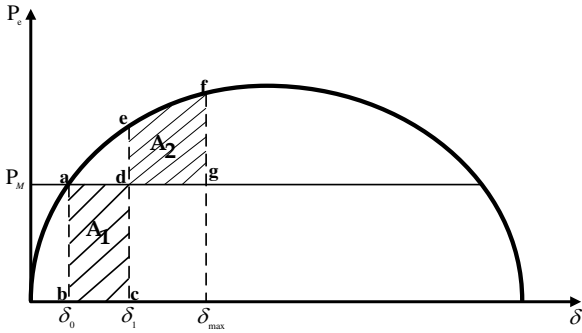


Figure 2. Equal Area Criterion (EAC) to determine the critical angle [4]

During the fault,  $P_e$  of the generator extremely reduces, but  $P_m$  almost remains constant. Thus, the generator accelerates and its angle  $\delta_0$  increases. If integrate from two hatched sides ( $A_1$  and  $A_2$ ),  $\delta_c$  obtained by Eq.(3):

$$\int_{\delta_0}^{\delta_c} P_m d\delta = \int_{\delta_c}^{\delta_{max}} (P_{max} \sin \delta - P_m) d\delta \quad (3)$$

where, the  $P_{max}$  is defined by Eq.(4):

$$P_{max_i} = \sum_{j=1}^m |E'_i| |E'_j| |Y_{ij}| \quad (4)$$

By solving Eq. (3):

$$P_m(\delta_c - \delta_0) = P_{max}(\cos \delta_c - \cos \delta_{max}) - P_m(\delta_{max} - \delta_c) \quad (5)$$

And  $\cos \delta_c$  equal to Eq.(6):

$$\cos \delta_c = \frac{P_m}{P_{max}}(\delta_{max} - \delta_c) + \cos \delta_{max} \quad (6)$$

where,  $\delta_0$  is the initial angle,  $\delta_{max}$  is the maximum angle that is equal to  $\pi - \delta_0$ , the critical angle of each generator. Now if a fault occurs on a generator's bus, the swing equation is solved for that generator and can be calculated for all generators in Eq. (7) and (8):

$$KE_i^{crit} = P_{M_i}(\delta_{c_i} - \delta_{0_i}) = \frac{1}{2} M_i (\bar{\omega}_{CRIT_i})^2 \quad (7)$$

$$v_{CRIT_i} = \sqrt{\frac{2KE_i^{crit}}{M_i}} \quad (8)$$

### 4. Transient Stability Using Direct Methods

Transient Energy Function (TEF) method is derived from the Lyapunov's method [2-5]. The transient energy approach can be described by a ball rolling on the inner surface of a bowl as shown in Figure 3. Initially, the ball is motionless which is equivalent to a power system in its steady-state equilibrium. When an external force is applied to the ball, the ball moves away from the equilibrium point. Equivalently, in a power system, a fault occurs in the system which causes the system to move away from the Stable Equilibrium Point (SEP). If the ball converts all its kinetic energy into potential energy before reaching the edge, then it will roll back and settle down at the new SEP eventually [4].

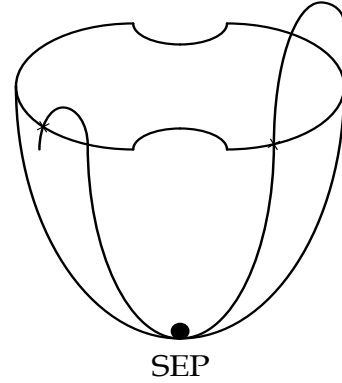


Figure 3. A ball rolling on the inner surface of a bowl [4]

When the fault is cleared, the gained Kinetic Energy (KE) is converted into Potential Energy (PE). This process continues until the initial KE is converted totally into PE causing the machine to converge toward the rest of the system. However, if the KE of machine  $i$  is not converted into PE, it loses synchronism and separates from the system and become unstable. Using formulas for KE and PE, we have an expression for the total energy of the system as follows in Eq. (9) :

$$V = \sum_{i=1}^n \int \frac{1}{2} M_i \bar{\omega}_i^2 d\omega_i - \sum_{i=1}^n \int P_i d\theta + \sum_{i=1}^{n-1} \sum_{j=i+1}^n C_{ij} \sin \theta_{ij} d\theta_{ij} + \int_{\theta_i^s + \theta_j^s}^{\theta_i + \theta_j} D_{ij} \cos \theta_{ij} d(\theta_i + \theta_j) \quad (9)$$

And then for each parts of equation (9), we have Eq. (10) and (11) :

$$\begin{aligned} \frac{1}{2} \sum_{i=1}^n M_i \bar{\omega}_i^2 &= \frac{1}{2} \sum_{i=1}^n M_i (\omega_i - \omega_0)^2 = \frac{1}{2} \sum_{i=1}^n M_i \omega_i^2 - \\ &\sum_{i=1}^n M_i \omega_i \omega_0 + \frac{1}{2} \sum_{i=1}^n M_i \omega_0^2 = \frac{1}{2} \sum_{i=1}^n M_i \omega_i^2 - M_T \omega_0^2 + \\ &\frac{1}{2} M_T \omega_0^2 = \frac{1}{2} \sum_{i=1}^n M_i \omega_i^2 - \frac{1}{2} \sum_{i=1}^n M_T \omega_0^2 \end{aligned} \quad (10)$$

$$\sum_{i=1}^n P_i (\theta_i - \theta_i^s) = \sum_{i=1}^n P_i (\delta_i - \delta_i^s) - [\sum_{i=1}^n P_i] (\delta_0 - \delta_0^s) \quad (11)$$

Now, if the excitation system and AVR, are taken into account [22], calculating the potential energy function and analyzing the stability is difficult because there are many dynamic and algebraic parameters that must be computed in

each repetition loop of time and are almost impossible to implement in real-time. On the other hand, the calculation of potential energy requires post-fault data.

Therefore, according to this explanation, in this paper, to analyze transient stability, a method has been proposed in which considering the network completely and it is possible to implement the proposed algorithm in a real-time simulator. In this method, transient stability analysis is done using the corrected kinetic energy function.

As can be seen, the calculation of PE is very complex and it needs the post-fault data; therefore, it is not appropriate for real-time applications. But, the presented index in this paper does not calculate potential energy and need post-fault data for transient stability assessment of the power system.

## 5. Proposed Method

### 5.1. Identification of Critical Machine Group (CMG)

The proposed method in the paper is based on the single-machine energy function that explained in the previous sections since the focus of this paper is on the classical model of the generator. The system is divided into CMG and NCMG. The selection procedure of the Critical Machine Group (CMG) in each disturbance depends on several parameters. By having system data at any time after occurring a fault in the system, the following procedure is used to select the CMG:

Step 1: A list of generators based on their kinetic energy at the end of each time step ( $\Delta t$ ), is arranged by descending order. Then only the generators are included on this list which their kinetic energy are more than 50% of the maximum kinetic energy of the list which is shown by Eq.(11):

$$CMG_{KE} = \{i: (\max(KE) - KE_i) < 0.5\max(KE)\} \quad (11)$$

Step 2: The second list of machines based on their acceleration at the end of each time interval ( $\Delta t$ ), is obtained (i.e. based on that is accelerator power for the  $i$ th generator at each time interval). This list also is arranged in descending order. Similar to the list of kinetic energy, only generators with acceleration higher than the 50% of the maximum acceleration are kept in the list which is shown by Eq.(12):

$$CMG_a = \left\{ i: \left( \max \left| \frac{d\omega}{dt} \right| - \left| \frac{d\omega_i}{dt} \right| \right) < 0.5 \max \left| \frac{d\omega}{dt} \right| \right\} \quad (12)$$

Step 3: Based on the above lists, the third list including generators in both lists is formed. In other words, it includes generators that are in the list of kinetic energy and acceleration as it is shown shown by Eq.(13):

$$CMG_{KE,a} = CMG_{KE} \cap CMG_a \quad (13)$$

The algorithm of finding CMG is shown in Figure 4.

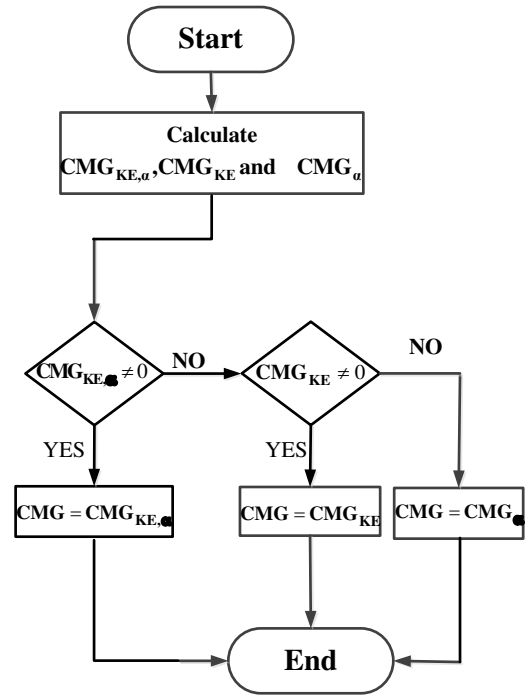


Figure 4. Finding Critical Machine Group (CMG) Algorithm

### 5.2. Corrected Kinetic Energy Function

Transient energy function after fault period is stored, nonetheless, all the transient kinetic energy is not turned into potential energy in the first swing of system separation [12-14]. Therefore, in various references such as reference[22-24], corrected kinetic energy is defined by Eq. (14) as follows:

$$KE^{CO} = \frac{1}{2} M_{eq} \omega^2 \quad (14)$$

where,  $M_{eq}$  and  $\bar{\omega}$  are defined by Eq. (15,16):

$$M_{eq} = \frac{M_{CMG} M_{NCMG}}{M_{CMG} + M_{NCMG}} \quad (15)$$

$$\omega = \omega_{CMG} - \omega_{NCMG} \quad (16)$$

$\omega_{NCMG}$  and  $\omega_{CMG}$  are defined by Eq. (17,18):

$$\omega_{NCMG} = \sum_i^{n_{sys}} \frac{M_i \bar{\omega}_i}{M_{NCMG}} \quad (17)$$

$$\omega_{CMG} = \sum_i^{n_{cr}} \frac{M_i \bar{\omega}_i}{M_{CMG}} \quad (18)$$

$M_{CMG}$  and  $M_{NCMG}$  are defined by Eq.(19,20):

$$M_{CMG} = \sum_{i=1}^{n_{CMG}} M_i \quad (19)$$

$$M_{NCMG} = \sum_{i=1}^{n_{NCMG}} M_i \quad (20)$$

### 5.3. Corrected Kinetic Energy Function

It should be noted that since all of the transient kinetic energy is not turned into potential energy in the first swing of separation of system, critical kinetic energy that was obtained for each generator also does not affect fully in the first swing of system separation and like that kinetic energy should be corrected as follows in Eq. (21):

$$KE_{crit}^{CO} = \frac{1}{2} M_{eq} \omega_{crit}^2 \quad (21)$$

where,  $\omega_{crit}$  is defined by Eq. 22:

$$\omega_{crit} = \omega_{crit}^{CMG} - \omega_{crit}^{NCMG} \quad (22)$$

$\omega_{crit}^{CMG}$  and  $\omega_{crit}^{NCMG}$  are defined by Eq. (23,24):

$$\omega_{crit}^{CMG} = \sum_{i=1}^{n_{cr}} \frac{M_i \bar{\omega}_{CRITi}}{M_{CMG}} \quad (23)$$

$$\omega_{crit}^{NCMG} = \sum_{i=1}^{n_{sys}} \frac{M_i \bar{\omega}_{CRITi}}{M_{NCMG}} \quad (24)$$

#### 5.4. Stability Margin Index

After calculating the corrected kinetic energy and the critical kinetic energy for any disturbance and interval ( $\Delta t$ ) can be expressed index to determine the stability margin of the system as follows in Eq. (25):

$$SMI = \frac{KE_{crit}^{CO}}{KE_{crit}^{CO}} = \frac{\frac{1}{2} M_{eq} \omega^2}{\frac{1}{2} M_{eq} \omega_{crit}^2} = \left( \frac{\omega}{\omega_{crit}} \right)^2 \quad (25)$$

The algorithm of Obtaining an index to determine the stability of the system for each interval ( $\Delta t$ ) is shown in Figure 5. In Figure 5, when the index is closer to 1, the system is close to instability, and when this index is closer to zero, the system is more stable.

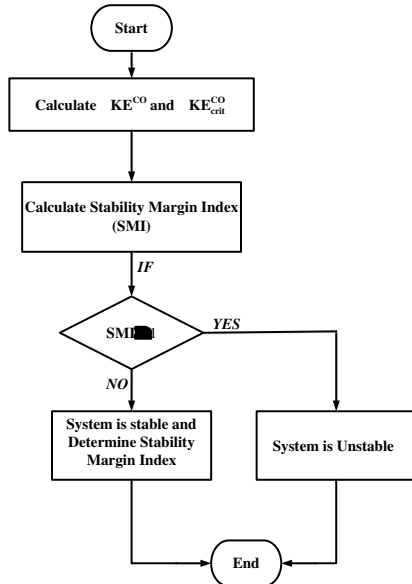


Figure 5. Achieving Stability Margin Index

## 6. Simulation and Results

To test the proposed method, IEEE 9 Bus test system is used to provide a comparison between kinetic and critical kinetic energies of a single machine. The test system contains 3 generators and 9 buses, as shown in Figure 6.

Generator and line data are listed in Table 1 and Table 2, respectively. Two different cases are simulated and the applied three-phase fault is severe enough to become system unstable and KE,  $\delta$ , and  $\omega$  for each generator and SF for the system are studied.

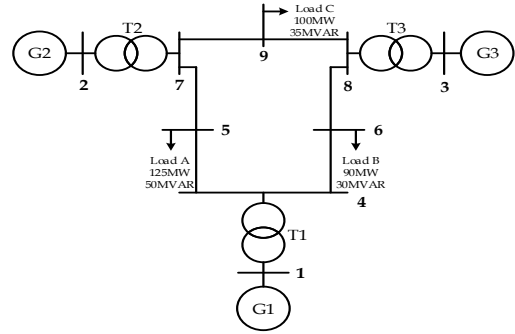


Figure 6. IEEE 9 bus test system

Table 1. Line data

Line data			
Line	Resistance	Reactance	Susceptance
1-4	0	0.0576	0
2-7	0	0.625	0
3-9	0	0.586	0
4-5	0.01	0.085	0.176
4-6	0.017	0.92	0.158
5-7	0.032	0.161	0.306
6-9	0.039	0.17	0.358
7-8	0.0085	0.072	0.149
8-9	0.0119	0.1008	0.209

Table 2. Generator data

Generator data			
Gen(i)	R	x <sub>D</sub> '	h
1	0	0.0608	23.64
2	0	0.1198	6.4
3	0	0.1813	3.01

#### 6.1. Case 1: (Fault Line 5-7 Near Bus5)

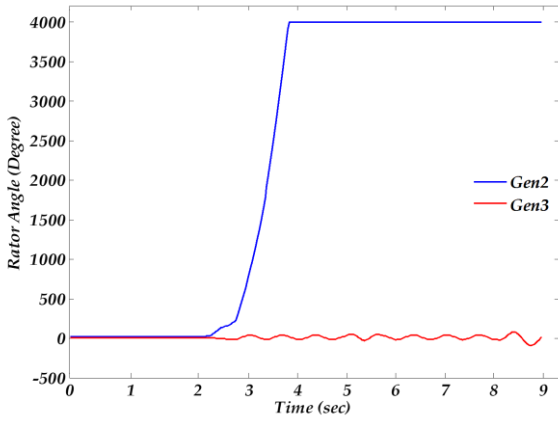
Since the synchronous reference frame is used, the speeds and angles are compared with the reference generator (slack).  $\delta_c$  and  $\omega_{crit}$  are computed by employing the EAC method and the previous equations; after the fault occurs at line 5-7 near bus 5 which is cleared after at 0.4 sec. Before transient stability assessment, load flow solution has been carried out to obtain initial values. These initial values are listed in Table 3 and Table 4. According to the Figures 7 and 8 can be found that the system will be unstable by this fault but did not specify the exact time of instability. With regards to Figure 9 that depicts SMI instability accurate time is clear. Figure 9 shows that the system is unstable before clearing fault means that the system has not the ability to absorb kinetic energy has been injected.

Table3. Results of load flow

Load Flow			
Gen(i)	E'(i)	delta0(i)	Pm(i)
1	1.063	2.2637	0.7182
2	1.0678	19.7042	1.63
3	1.0262	13.0971	0.85

**Table 4.** Critical values

Critical values			
Gen(i)	E'(i)	delta0(i)	Pm(i)
1	1.063	2.2637	0.7182
2	1.0678	19.7042	1.63
3	1.0262	13.0971	0.85



**Figure 7.** Rotor's angles when fault occurs in bus 5, clear after 0.4 sec

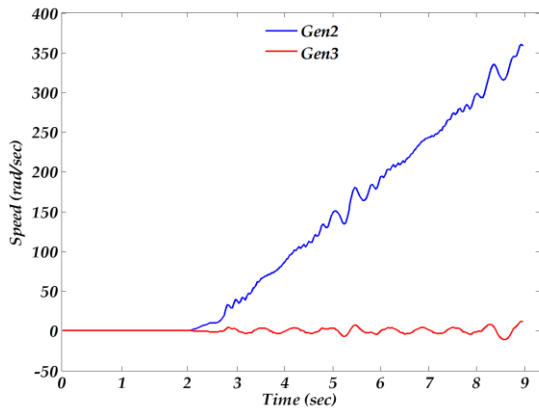


**Figure 8.** Rotor's speeds when fault occurs in bus 5, clear after 0.4 sec

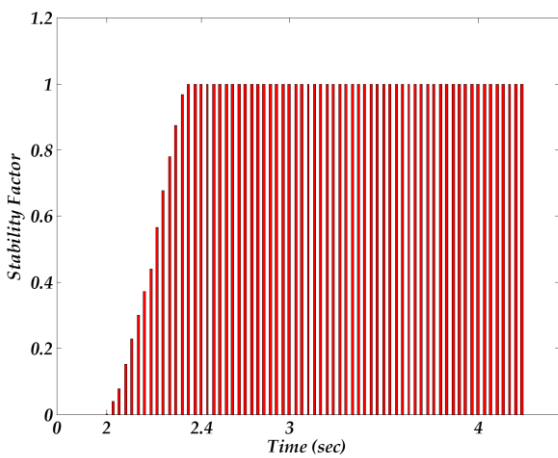


**Figure 9.** SMI when the fault occurs in bus 5, clear after 0.4 sec.

6.2. Case2: (Fault at Line 6-8 Near Bus8)

In this case fault occurs at line 6-8 near bus 8 and clear after 0.2 sec, we can see various  $\delta$  and  $\omega$  for each generator and SMI for the system. It can be realized According to figures 10, 11, and 12 the system is stable, but the stability margin and how much the system is close to instability cannot be found.

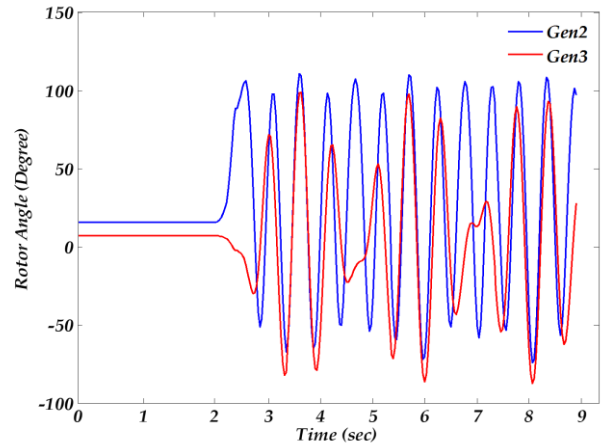


**Figure 10.** Rotor's angles when the fault occurs in bus 8, clear after 0.3 sec.

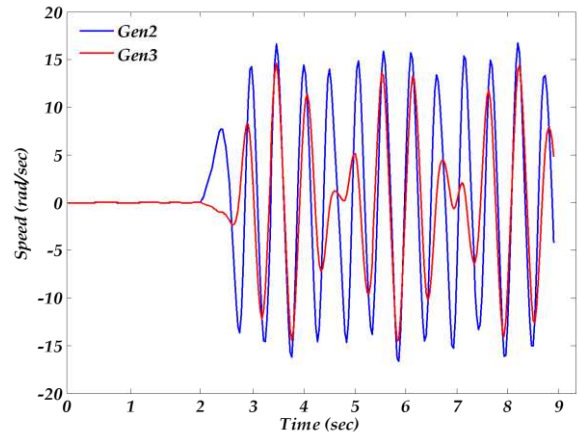


**Figure 11.** Rotor's speeds when the fault occurs in bus 8, clear after 0.3 sec

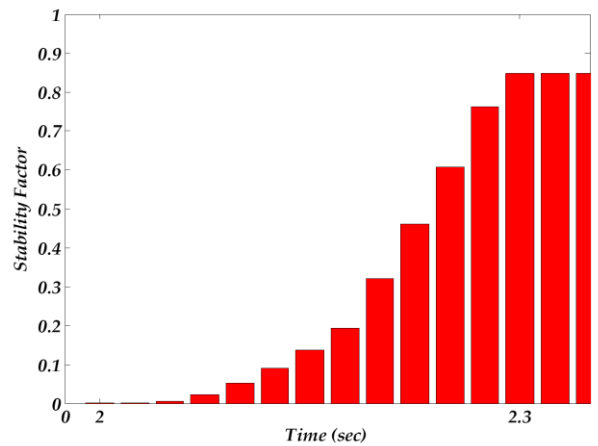


**Figure 12.** SMI when the fault occurs in bus 8, clear after 0.3 sec.

## 7. Conclusions

The proposed method is based on transient energy function methods, which can be used to determine transient stability directly without solving the power system equations numerically. It uses the energy conversion phenomena for any object. Due to problems in obtaining potential energy function, an index was introduced to determine the stability margin system used to kinetic energies term. The method uses the critical kinetic and kinetic energies which are compared with each other. If the critical kinetic energy is greater than the kinetic energy, then the system is considered unstable and if the kinetic energy is greater than the critical kinetic energy system is stable and determines the stability margin of the system. The proposed method is applied to the IEEE 9 Bus power system for several fault cases.

## References

- [1] C.-W. Liu, M.-C. Su, S.-S. Tsay, and Y.-J. Wang, "Application of a novel fuzzy neural network to real-time transient stability swings prediction based on synchronized phasor measurements," *IEEE Transactions on Power Systems*, vol. 14, pp. 685-692, 1999.
- [2] R. Evans and C. Wagner, "Studies of transmission stability," *Transactions of the American Institute of Electrical Engineers*, vol. 45, pp. 51-94, 1926.
- [3] P. Kundur, N. J. Balu, and M. G. Lauby, *Power system stability and control* vol. 7: McGraw-hill New York, 1994.
- [4] V. Vittal and A. Bergen, "Power systems analysis," *Prentice Hall*, pp. 1-2, 1999.
- [5] P. C. Magnusson, "The transient-energy method of calculating stability," *Transactions of the American Institute of Electrical Engineers*, vol. 66, pp. 747-755, 1947.
- [6] H. Al Marhoon, I. Leevongwat, and P. Rastgoufard, "A practical method for power systems transient stability and security analysis," in *PES T&D 2012*, 2012, pp. 1-6.
- [7] A. Michel, A. Fouad, and V. Vittal, "Power system transient stability using individual machine energy functions," *IEEE Transactions on Circuits and Systems*, vol. 30, pp. 266-276, 1983.
- [8] Q. Jiang and Z. Huang, "An enhanced numerical discretization method for transient stability constrained optimal power flow," *IEEE Transactions on Power Systems*, vol. 25, pp. 1790-1797, 2010.
- [9] C. Wang, K. Yuan, P. Li, B. Jiao, and G. Song, "A projective integration method for transient stability assessment of power systems with a high penetration of distributed generation," *IEEE Transactions on Smart Grid*, vol. 9, pp. 386-395, 2016.
- [10] A. Priyadi, N. Yorino, O. A. Qudsi, and M. H. Purnomo, "CCT computation method based on critical trajectory using simultaneous equations for transient stability analysis," in *2014 6th International Conference on Information Technology and Electrical Engineering (ICITEE)*, 2014, pp. 1-6.
- [11] M. Pavella, D. Ernst, and D. Ruiz-Vega, *Transient stability of power systems: a unified approach to assessment and control*: Springer Science & Business Media, 2012.
- [12] Y. Xue, T. Van Cutsem, and M. Ribbens-Pavella, "Extended equal area criterion justifications, generalizations, applications," *IEEE Transactions on Power Systems*, vol. 4, pp. 44-52, 1989.
- [13] S. Mahdavi and A. Dimitrovski, "Coordinated voltage regulator control in systems with high-level penetration of distributed energy resources," in *2019 North American Power Symposium (NAPS)*, 2019, pp. 1-6.
- [14] S. Mahdavi and A. Dimitrovski, "Integrated Coordination of Voltage Regulators with Distributed Cooperative Inverter Control in Systems with High Penetration of DGs," in *2020 IEEE Texas Power and Energy Conference (TPEC)*, 2020, pp. 1-6.
- [15] N. Sarikhani and A. G. Mazidi, "Online Distribution System's Voltage Stability Margin Monitoring Using Neural Networks and Optimization Algorithm," *Computational Research Progress in Applied Science & Engineering*, vol. 2, pp. 23-27, 2016.
- [16] H. P. S. Mahdavi, A. Dimitrovski and Q. Zhou, "Predictive and Cooperative Voltage Control with Probabilistic Load and Solar Generation Forecasting," in *2020 IEEE International Conference on Probabilistic Methods Applied to Power Systems (PMAPS)*, Liege, Belgium, 2020, pp. 1-6.
- [17] H. Shokouhandeh, M. Ghaharpour, H. G. Lamouki, Y. R. Pashakolaei, F. Rahmani, and M. H. Imani, "Optimal Estimation of Capacity and Location of Wind, Solar and Fuel Cell Sources in Distribution Systems Considering Load Changes by Lightning Search Algorithm," in *2020 IEEE Texas Power and Energy Conference (TPEC)*, 2020, pp. 1-6.
- [18] R. P. A. Taghavirashidizadeh, M. Hayerikhiyavi, M. Zahedi, "A Genetic Algorithm for Multi-Objective Reconfiguration of Balanced and Unbalanced Distribution Systems in Fuzzy Framework," *Journal of Critical Reviews*, vol. 7(7), pp. 639-343, 2020.
- [19] F. Milano, "An open source power system analysis toolbox," *IEEE Transactions on Power systems*, vol. 20, pp. 1199-1206, 2005.
- [20] P. M. Anderson and A. Fouad, *Power system stability*: Wiley-IEEE Press, 2003.
- [21] A. Pizano-Martianez, C. R. Fuerte-Esquivel, and D. Ruiz-Vega, "Global transient stability-constrained optimal power flow using an OMIB reference trajectory," *IEEE Transactions on Power Systems*, vol. 25, pp. 392-403, 2009.
- [22] A. Vahidnia, G. Ledwich, E. Palmer, and A. Ghosh, "Dynamic equivalent state estimation for multi-area power systems with synchronized phasor measurement units," *Electric power systems research*, vol. 96, pp. 170-176, 2013.
- [23] R. F. Gibson, E. O. Ayorinde, and Y.-F. Wen, "Vibrations of carbon nanotubes and their composites: a review," *Composites science and technology*, vol. 67, pp. 1-28, 2007.
- [24] H. Richter, D. Simon, W. A. Smith, and S. Samorezov, "Dynamic modeling, parameter estimation and control of a leg prosthesis test robot," *Applied Mathematical Modelling*, vol. 39, pp. 559-573, 2015.